Correlation between the extraordinary Hall effect and resistivity

A. Gerber, A. Milner, A. Finkler, M. Karpovski, and L. Goldsmith
Raymond and Beverly Sackler Faculty of Exact Sciences, School of Physics and Astronomy, Tel Aviv University, Ramat Aviv, 69978 Tel Aviv, Israel

J. Tuaillon-Combes, O. Boisron, P. Mélinon, and A. Perez
Laboratoire de Physique de la Matière Condensée et Nanostructures, Université Claude Bernard Lyon 1, F-69622 Villeurbanne, France
(Received 28 May 2003; revised manuscript received 3 December 2003; published 7 June 2004)

We propose to reconsider the correlation between the extraordinary Hall effect and resistivity by using the skew scattering model and Matthiesen's rule to separate contributions of different scattering sources. The model has been experimentally tested for the cases of scattering by magnetic nanoparticles embedded in normal-metal matrix, insulating impurities in magnetic matrix, surface scattering, and temperature-dependent scattering.

DOI: 10.1103/PhysRevB.69.224403 PACS number(s): 75.47.−m, 72.15.Qm, 73.50.−h

I. INTRODUCTION

The anomalous or extraordinary Hall effect (EHE) in magnetic materials has remained a poorly understood phenomenon since its discovery more than a century ago. Phenomenology of the effect is straightforward. Hall resistivity ρ_H in magnetic materials is described as: $\rho_H = R_0 B + R_{EHE}\mu_0 M$, where the first term presents an ordinary Hall effect, related to the Lorentz force acting on moving charge carriers, and the second term presents the extraordinary Hall effect with M being the macroscopic magnetization and R_{EHE} the extraordinary Hall effect coefficient. Correlation between the Hall signal and magnetization is well established and has been used for a variety of applications.[1,2] Problems arise when theoretical models are confronted by experimental data, for example, when correlation between the EHE and resistivity is discussed.

The EHE is, in many cases, much larger than the ordinary Hall effect and is generally believed to originate from a spin-dependent scattering that breaks a spatial symmetry in the trajectory of scattered electrons. It has been recently proposed that there is an additional contribution of the order of magnitude comparable to that of the ordinary Hall effect and independent of any scattering.[3] Some models assume the carriers to be magnetic and the scattering centers nonmagnetic,[4–6] while in others the situation is reversed.[7,8] Since scattering is responsible both for EHE and longitudinal resistivity, link between two parameters is usually claimed.

Two types of scattering events are distinguished in the EHE literature.[9] One is referred to as skew scattering and is characterized by a constant spontaneous angle θ_s at which the scattered carriers are deflected from their original trajectories. The predicted[9,10] correlation between the EHE coefficient and resistivity is: $R_{EHE} = A\rho + B\rho^2$. The second term is frequently neglected and a linear ratio between R_{EHE} and ρ is mentioned. The other scattering mechanism, so-called side jump, is quantum mechanical in nature and results in a constant lateral displacement Δy of the charge's trajectory at the point of scattering. For the side jump mechanism $R_{EHE} \propto \rho^2$. Because of the different dependence on resistivity of these mechanisms the EHE is usually attributed to the skew scattering when ρ is small (low temperatures and / or pure metals) and to the side jump when ρ is large (high temperatures, concentrated alloys, and disordered materials). Superposition of two mechanisms is presented as

$$R_{EHE} = a\rho + b\rho^2, \tag{1}$$

where the first term is believed to relate to the skew scattering and the second to the side jump mechanism with a possible contribution of the skew scattering as well. A simplified alternative form of presentation is $R_{EHE} = \alpha\rho^n$ with $n=1$ corresponding to skew scattering, $n=2$ to the side jump, and intermediate values $1<n<2$ accepted as a superposition of two mechanisms.

Unfortunately, much of the experimental data fall far from theoretical expectations including, most notoriously, cases in which the power index n is found to exceed 2. It has been recently argued[11–13] that in heterogeneous systems, where the mean-free path is comparable or greater than the topological modulation length, the simple scaling relationship between R_{EHE} and ρ no longer holds. The Hall resistivity in heterogeneous systems depends on the ratio of relaxation times (mean-free paths) in magnetic and nonmagnetic regions and as a result the power n may be smaller or greater than 2. These arguments have been used to justify higher than two power-law values found in, e.g., Fe/Cr multilayers[14] ($n=2.6$) and granular films of Co-Ag (Ref. 15) ($n=3.7$). However, significant discrepancies, including $n>2$, have been found much earlier not only in heterogeneous but also in bulk homogeneous systems.[16–18]

We, therefore, propose to reconsider the very correlation between the EHE and resistivity. The present work is an attempt to abandon the traditional link between the *total values* of two parameters. Instead, we decompose both EHE and resistivity to contributions generated by different scattering sources and follow the correlation for each source independently.

II. MODEL

Let us start with a simple modification of the skew scattering model. Let us assume that only a certain type of scat-

tering event gives rise to skew scattering, the rest do not break the scattering symmetry. We shall call the sources which generate skew scattering as "skew" and the rest as "ballast." Let us also assume that the total resistivity ρ follows the Matthiesen's rule $\rho=\rho_0+\rho_s$, where ρ_s is the contribution of skew sources and ρ_0 is due to the ballast scattering events. Justification of this assumption will be discussed later. ρ_s and ρ_0 can be further subdivided if more than two sources are involved. We consider the system in high applied magnetic field with all magnetic moments saturated and aligned along the field. The EHE resistivity in this saturated state is field independent and we denote it as ρ_{EHE}. Transverse current density $J_\perp$ generated by electrons deflected by skew scattering is proportional to the volume density of skew centers n_s: $J_\perp=\alpha n_s J$, where J is the longitudinal current density. Coefficient α is proportional to the skew angle θ_s. Transverse electric field $E_\perp$ is: $E_\perp=J_\perp\rho=\alpha n_s J\rho=\alpha n_s J(\rho_0+\rho_s)$, and Hall resistivity ρ_{EHE} is thus given by

$$\rho_{EHE}=E_\perp/J=\alpha n_s(\rho_0+\rho_s). \tag{2}$$

If $\rho_s\propto n_s$, Eq. (2) can be rewritten as

$$\rho_{EHE}=\gamma\rho_0\rho_s+\gamma\rho_s^2, \tag{3}$$

where γ is coefficient.

Equations (2) and (3) allow us to analyze the correlation between the measured Hall resistivity and scattering components by varying only one source at time. If ρ_s is kept constant, ρ_{EHE} is expected to be a linear function of ρ_0 with a slope proportional to ρ_s and residual value $\gamma\rho_s^2$ at $\rho_0=0$. If ρ_0 is kept constant and the skew scattering term ρ_s is varied, ρ_{EHE} becomes a sum of linear and quadratic terms of ρ_s with the coefficient of the linear term proportional to ρ_0. Contrary to Eq. (1), both linear and quadratic terms originate from the same skew scattering mechanism only.

In the following section we present several experiments in which different scattering mechanisms have been varied in a controllable way.

III. EXPERIMENTAL RESULTS AND DISCUSSION

A. Magnetic scattering centers

Correlation between the EHE resistivity and density of magnetic scattering centers has been studied in a series of dilute planar arrays of Co nanoclusters embedded in Pt matrix. The samples were produced by the low-energy clusters beam deposition technique.[19,20] The Co clusters are crystalline in FCC-phase with a narrow distribution of diameters of approximately 3 nm. Under and over layers of Pt films of 5 and 15 nm, respectively, were deposited from an electron gun evaporator mounted in the same deposition chamber. The mean thickness of the Co clusters t, defined as a total deposited mass divided by density of Co, varied by two orders of magnitude between 0.01 and 1.1 nm. Position of Co clusters in an array is random with an average center-to-center distance L estimated as $L=a^{3/2}/(2t)^{1/2}$, where a is diameter of clusters. L, therefore, is calculated to vary in our samples between 37 and 3.5 nm.

The films are nanocrystalline and their overall resistivity is mainly due to boundary scattering. Substitution of Pt crystallites by Co nanoclusters has no visible effect on the total resistivity of the entire series, which is of the order of 40 $\mu\Omega$ cm at room temperature. On the other hand, the Hall resistivity depends strongly on the concentration of Co clusters. Typical variation of the Hall resistivity with respect to the applied magnetic field is shown in Fig. 1 for three samples with effective Co thicknesses of 0.1, 0.5, and 1 nm, as measured at room temperature. The samples are superparamagnetic with the blocking temperature at about 40 K. Hysteresis is developed in $\rho_H(B)$ curve below this temperature. ρ_{EHE}, the saturated extraordinary Hall resistivity, can be found by extrapolating the high-field linear slope of $\rho_H(B)$ to zero field. Figure 2 presents the EHE resistivity plotted as a function of Co-clusters planar density n_s. ρ_{EHE} increases linearly with n_s in agreement with Eq. (2) for $\rho=\rho_0+\rho_s=$const.

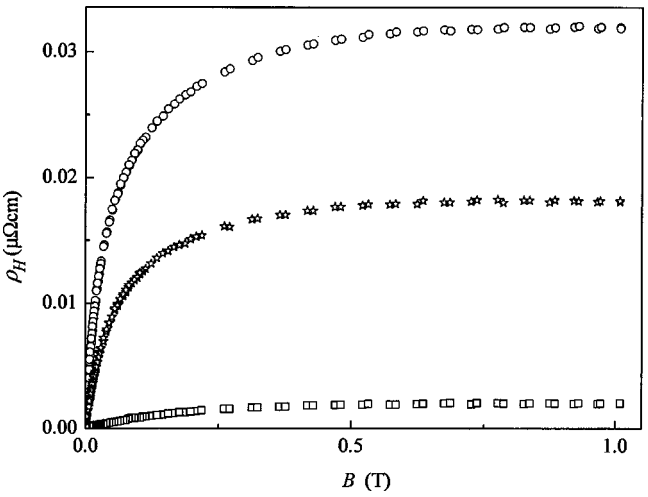

FIG. 1. Hall resistivity of three planar arrays of Co nanoclusters embedded in Pt matrix as a function of the applied magnetic field. Mean thickness of Co is 0.1 nm (squares), 0.5 nm (stars), and 1 nm (circles). $T=290$ K.

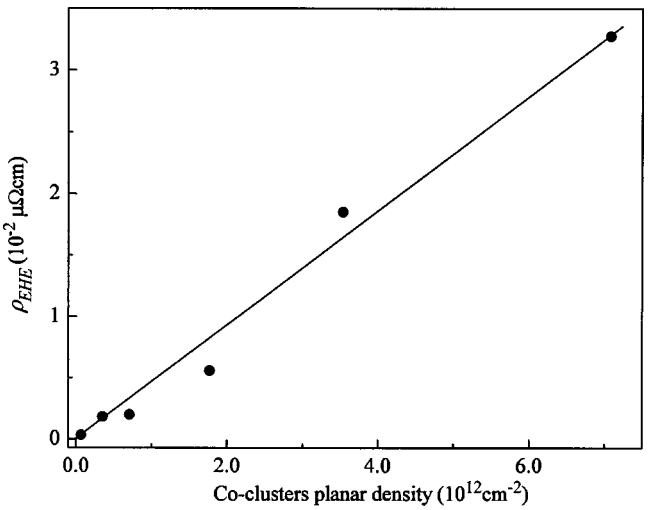

FIG. 2. The saturated EHE resistivity of planar arrays of Co nanoclusters embedded in Pt matrix as a function of Co-clusters planar density. Solid line is the guide for eyes.

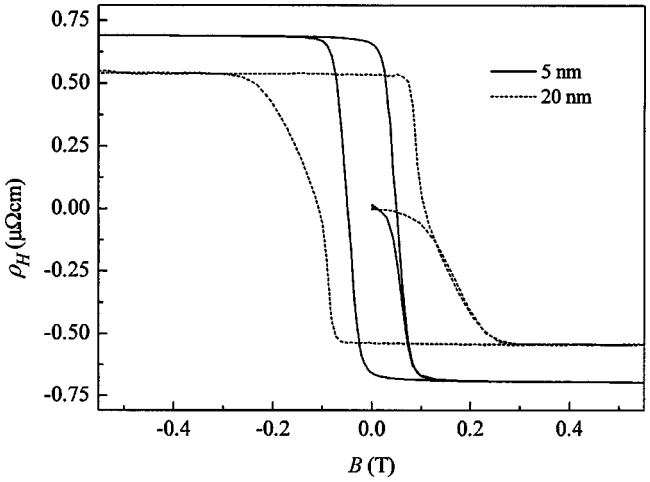

FIG. 3. Hall resistivity of two thin Ni films with thickness of 5 nm (solid line) and 20 nm (dotted line) as a function of the applied magnetic field. $T=4.2$ K.

B. Surface scattering

The effect of surface scattering on EHE has been studied[21] in series of thin Ni films with thickness of the order of the electronic mean-free path. Typical dependence of the Hall resistivity on the applied magnetic field is shown in Fig. 3 for two films with thickness of 5 nm (solid line) and 20 nm (dotted line) measured at 4.2 K. Following the Fuchs-Sondheimer[22] size effect model, external surfaces impose a boundary condition on the electron-distribution function, which enhances the intrinsic, thickness independent bulk resistivity ρ_b to a thickness-dependent resistivity ρ. The total longitudinal resistivity ρ and the extraordinary Hall resistivity ρ_{EHE} of a typical series of Ni films measured at room temperature is plotted in Fig. 4 as a function of film's thickness. Both resistivities are constant in samples thicker than 100 nm and the latter is taken as the bulk value. The surface scattering term can be extracted explicitly as $\rho_{ss}=\rho-\rho_b$. In a similar way, the contribution of surface scattering to the EHE resistivity can be found as $\rho_{EHEss}=\rho_{EHE}-\rho_{EHEb}$,

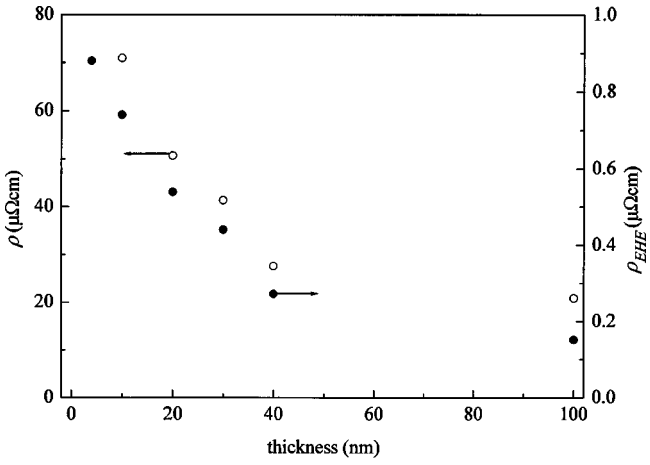

FIG. 4. Longitudinal (ρ) and EHE (ρ_{EHE}) resistivity of a series of thin Ni films as a function of their thickness. $T=290$ K.

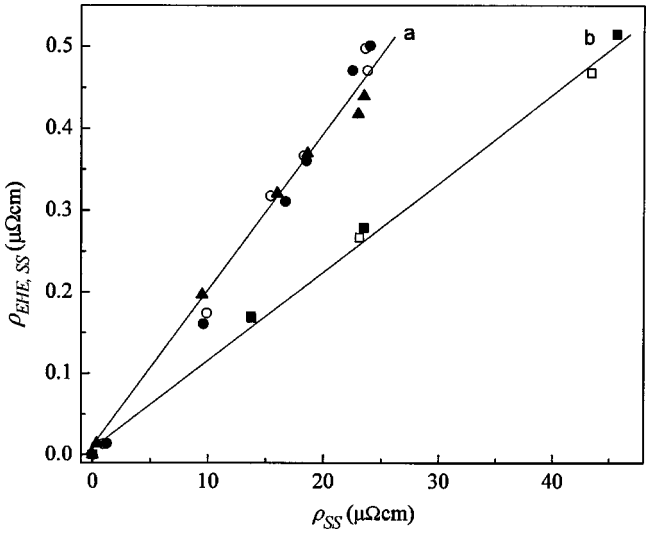

FIG. 5. Contribution of the surface scattering to the EHE resistivity of thin Ni films as a function of the respective contribution to longitudinal resistivity. Series (*a*) has been measured at three temperatures: 4.2 K, 77 K, and 290 K, and series (*b*) at 77 K and 290 K. Solid lines are the guides for eyes.

where ρ_{EHE} and ρ_{EHEb} are the EHE resistivity of a given film and bulk, respectively. Figure 5 presents ρ_{EHEss} as a function of ρ_{ss} for two sets of Ni films prepared under different deposition conditions [resistivity of the thick sample in series (*b*) is about three times higher than that in series (*a*)]. Series (*a*) has been measured at three temperatures: 4.2 K, 77 K, and 290 K, and series (*b*) at 77 K and 290 K. The variation is independent of temperature and is linear for both series. It is in agreement with Eqs. (2) and (3) for the case in which the ballast resistivity is varied and the skew subsystem is kept constant.

C. Insulating nonmagnetic impurities

The case of insulating nonmagnetic impurities has been tested by adding silica into nickel. Series of Ni-SiO_2 films were prepared by codeposition of Ni and SiO_2 in a two-gun *e*-beam deposition chamber. More details on fabrication of this type of material have been reported elsewhere.[23] Morphology of disordered mixtures, such as Ni-SiO_2, changes dramatically as a function of SiO_2 concentration. The size of silica clusters increases, fractal structure is developed and, finally, the percolation threshold is reached. In the present experiment we tried to avoid these complications and limited the concentration of SiO_2 to a few volume percents only, such that Ni matrix was kept far above the percolation threshold. Resistivity generated by SiO_2 inclusions has been defined as: $\rho_{SiO_2}=\rho-\rho_{Ni}$, where ρ is resistivity of a given sample and ρ_{Ni} is resistivity of a pure Ni sample prepared in the same deposition conditions and measured at the same temperature. The contribution of SiO_2 impurities to the EHE resistivity is calculated in a similar way as: $\rho_{EHE,SiO_2}=\rho_{EHE}-\rho_{EHE,Ni}$ with the same meaning of indices. ρ_{EHE,SiO_2} is plotted as a function of ρ_{SiO_2} in Fig. 6 for 77 K and 290 K. Similar to the case of surface scattering, the result is consis-

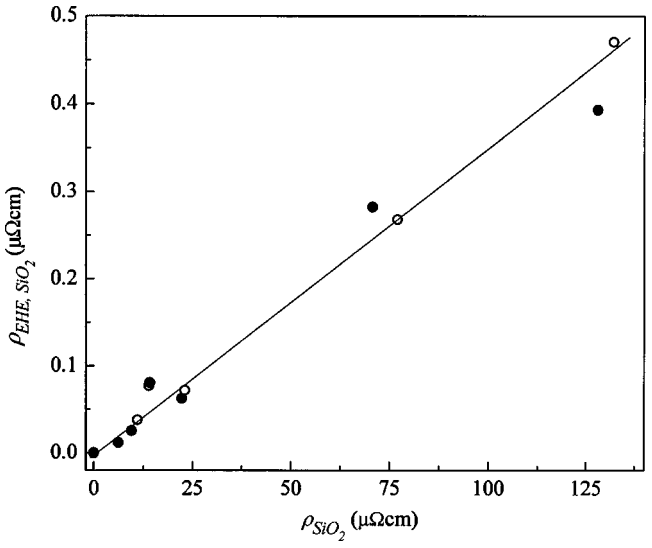

FIG. 6. Contribution of SiO_2 impurities to the EHE resistivity of a series of Ni-SiO_2 films as a function the respective contribution to longitudinal resistivity. $T=290$ K, open circles; and $T=77$ K, solid circles. Solid line is the guide for eyes.

tent with the situation in which skew subsystem is kept constant and ballast resistivity is modified.

D. Temperature-dependent scattering

Correlation between the temperature-dependent components of the EHE coefficient and resistivity has been studied using dilute planar arrays of Co nanoparticles embedded in Pt matrix. Dilute arrays with $a=3$ nm and mean thickness $t=0.1, 0.05$, and 0.01 nm, corresponding to average intercluster spacing of about 11.6 nm, 16.4 nm, and 36.7 nm, respectively, demonstrate identical normalized $\rho_H(B)$ curves, which indicates that the density of Co clusters is sufficiently low to avoid their coupling. Magnetization of thick samples prepared by codeposition of Co clusters and Pt matrix in the same installation and by the same technique we used has been measured by vibrating-sample magnetometer and reported in Ref. 20. Correlation between magnetization and the EHE resistivity in dilute samples is demonstrated in Fig. 7. Here, magnetization of the thick Co-Pt sample, reproduced from Ref. 20 (4% volume of Co corresponding to $L\approx 7$ nm) is plotted together with the EHE component of the Hall resistivity $\rho_H(B)$, measured in a planar array with a mean Co thickness of 0.05 nm ($L\approx 16.4$ nm). Both axes are, respectively, normalized. Results are shown for two temperatures: 1.5 K and 150 K. Correlation between two types of measurements is perfect which allows us to use the magnetization data to calculate the extraordinary Hall effect coefficient $R_{EHE}(T)$ as: $R_{EHE}(T)=\rho_{EHE}(T)/\mu_0 M_{sat}(T)$, where $M_{sat}(T)$ is the saturated high-field magnetization reported in Ref. 20. (Exact matching of the reference magnetization and EHE resistivity is found in all dilute arrays regardless their concentration, as expected for systems with uncorrelated magnetic clusters.)

The extraordinary Hall effect coefficient $R_{EHE}(T)$ is plotted in Fig. 8 for the Co-Pt sample with a mean Co thickness

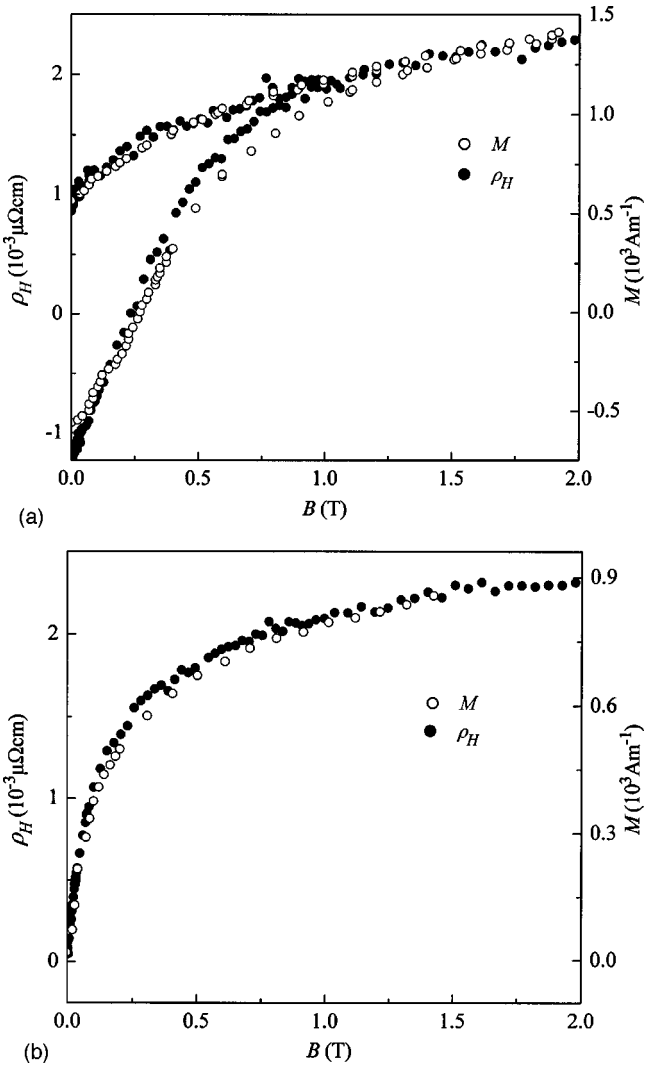

FIG. 7. The EHE component of the Hall resistivity $\rho_H(B)$, measured in a planar array with a mean Co thickness of 0.05 nm ($L\approx 16.4$ nm)— (left-side axis, solid dots) and magnetization of the thick Co-Pt sample (4% volume of Co corresponding to $L\approx 7$ nm)— (right-side axis, open circles) as a function of the applied magnetic field at (a) 1.5 K and (b) 150 K. Magnetization data are reproduced from Ref. 20.

of 0.05 nm ($L\approx 16.4$ nm) between 1.5 K and room temperature. The temperature dependence of resistivity is shown in the same temperature range in Fig. 9. Both ρ and R_{EHE} behave similarly as a function of temperature: they saturate to the residual value at low temperatures and increase gradually when the sample is heated.

Prior to focusing on the extracted temperature-dependent components of the EHE and longitudinal resistivity, it is illuminating to view a traditional presentation of the total R_{EHE} as a function of the total ρ in linear and log-log plots when temperature is varied. In addition to our results with Ni and Co-Pt samples, we reproduce several sets of data reported earlier for a range of magnetic materials. These include thin films of iron (19 and 75 nm thick),[24] polycrystalline iron films,[25] Ni films,[26] sputtered Pt/Au/Co/Pt sandwiches,[27] Fe/Cr multilayers with variable interfacial

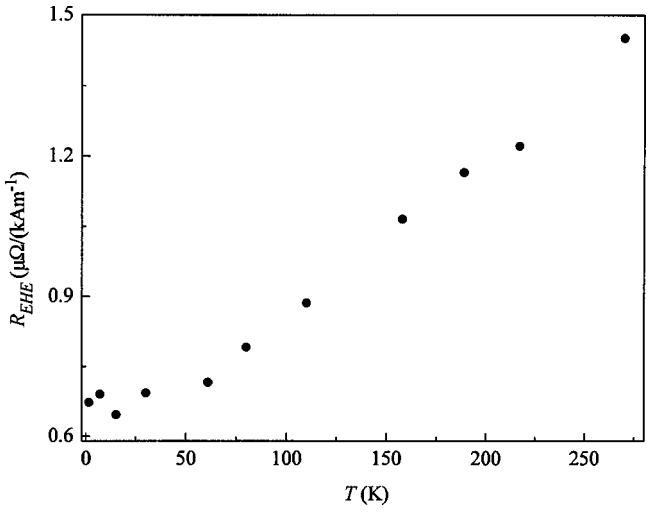

FIG. 8. Temperature dependence of the EHE coefficient R_{EHE} of the Co-Pt array sample with the mean Co thickness of 0.05 nm ($L \approx 16.4$ nm).

roughness,[28] textured Fe/Cr multilayers grown by electron-beam evaporation[14], Co/Cu superlattices,[29] and Fe-Ag granular alloys.[30] Two latter systems demonstrate large magnetoresistance and we refer to their resistivity in the saturated high-field state. R_{EHE} of all the mentioned materials, normalized by their maximal values at the highest reported temperatures (room temperature in most cases) is plotted in Fig. 10(a) as a function of the respective resistivity. The same data in log-log scale is shown in Fig. 10(b) with resistivity of each sample normalized by its highest value. Distribution of slopes in the latter plot, identified with power indices n, is disturbingly wide: from 0.8 in one of Pt/Au/Co/Pt sandwiches[27] to 2.6 in Fe/Cr multilayers.[14]

The temperature-dependent components ρ_{th} and $R_{EHE,th}$ have been extracted by subtracting the respective residual values at the lowest measured temperatures. The resulting $R_{EHE,th}$ normalized by their maximal values at the highest reported temperature is plotted in Fig. 11 as a function of the,

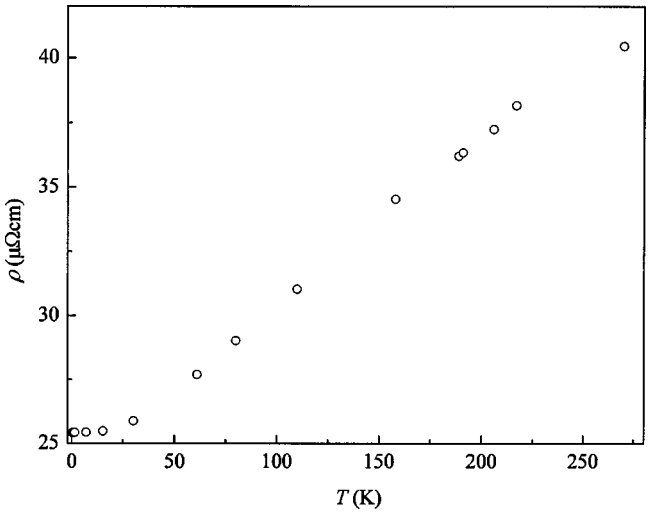

FIG. 9. Temperature dependence of resistivity of the Co-Pt array sample with the mean Co thickness of 0.05 nm ($L \approx 16.4$ nm).

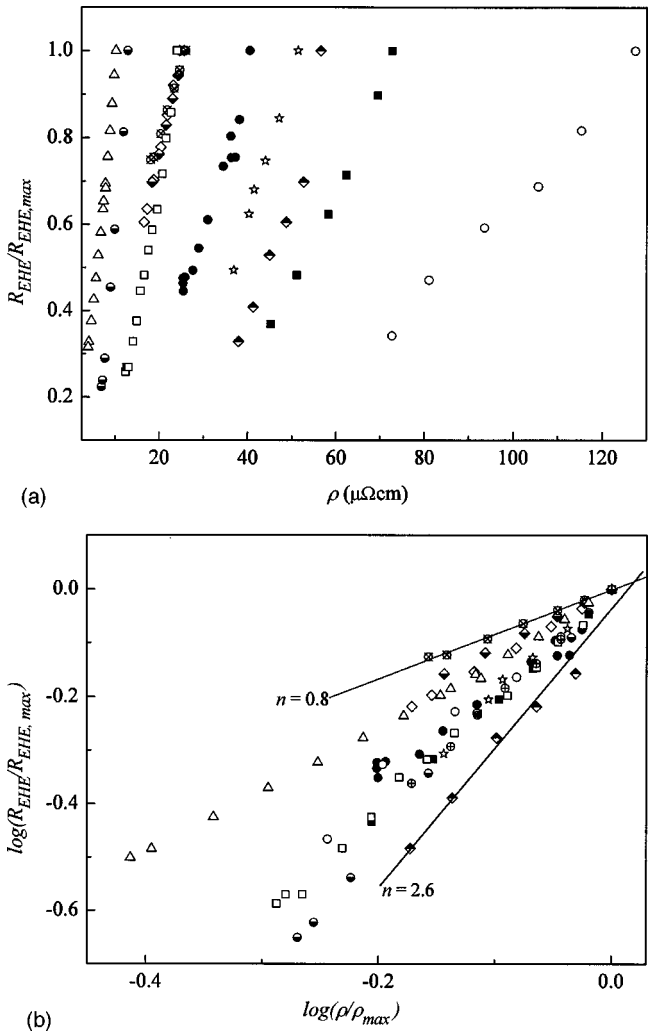

FIG. 10. Normalized values of the total EHE coefficient R_{EHE} as a function of the total resistivity ρ (a); and as a function of the respectively normalized total resistivity ρ in log-log scale (b), measured at different temperatures. Symbols indicate: •, Co-Pt arrays; ♦, Fe-Cr multilayers (Ref. 5); ☆, Fe-Ag granular alloys (Ref. 19); ◇, ⬙, ⊗, three Pt/Au/Co/Pt sandwiches (Ref. 16); ■,○, Fe, films (19 and 75 nm thick) (Ref. 13); △, Ni films (Ref. 15); □, Co-Cu superlattice (Ref. 18); ◒, polycrystalline Fe films (Ref. 14); ⊕, Fe-Cr multilayers (Ref. 17).

respectively, normalized ρ_{th}. All sets of data seem to collapse along a straight line, which means that for each of these materials the ratio between the temperature-dependent components of the extraordinary Hall coefficient and resistivity is close to be constant. It should be noted that this result is not a trivial consequence of a possible smallness of, e.g., $R_{EHE,th}$ as compared with $R_{EHE}(T=0)$. In fact, R_{EHE} varies significantly with temperature [see Fig. 10(a)], the ratio between the helium and room temperature values is about 0.3 in, e.g., Fe (Ref. 24) and Co-Cu superlattices,[29] 0.5 in Fe-Ag granular alloys[30] and our Co-Pt arrays; and 0.7 in Pt/Au/Co/Pt sandwiches.[27] The range of resistivity is also wide [Fig. 10(a)]: resistivity of Ni (Ref. 26) increases from about 4 to 12 $\mu\Omega$ cm, Co-Pt array from 25 to 40 $\mu\Omega$ cm, and 19 nm thick Fe film[24] from 70 to 130 $\mu\Omega$ cm.

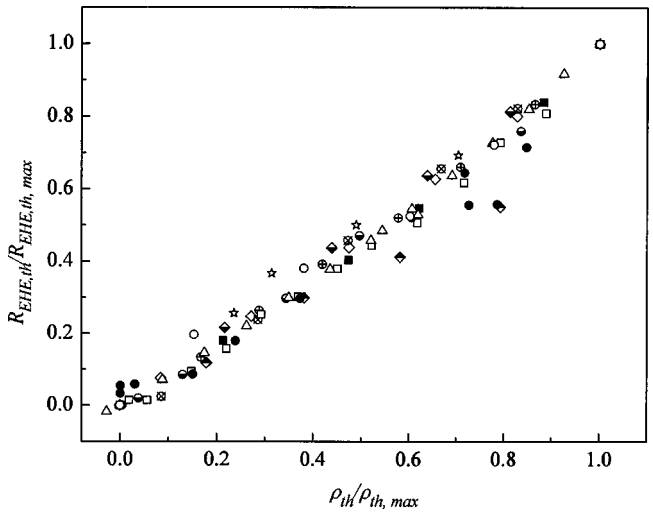

FIG. 11. Normalized values of the temperature-dependent component of the EHE coefficients $R_{EHE,th}$ as a function of the respectively normalized values of the temperature-dependent term of resistivity ρ_{th}. Symbols indicate the same selection of materials as in Fig. 10.

Seemingly universal linear variation of $R_{EHE,th}$ with ρ_{th} manifested in Fig. 11 should be taken with caution. In majority of cases, $R_{EHE,th}$ is fitted better by a two term expression

$$R_{EHE,th} = a\rho_{th} + b\rho_{th}^2, \tag{4}$$

where the absolute values of b are much smaller than a. If, alternatively, $R_{EHE,th}$ is presented as $R_{EHE,th}=c\rho_{th}^n$, the power index n varies between $n=0.9$ in Fe-Ag granular alloys,[30] to $n=1.2$ in Co/Cu superlattices[29] and iron films,[24] which can be interpreted as a dominance of the linear term $a\rho_{th}$. In some cases deviation of $R_{EHE,th}$ vs ρ_{th} from linearity is significant, e.g., in Co/Pt superlattices reported by Canedy *et al.*[31], and the quadratic term $b\rho_{th}^2$ cannot be neglected. In the framework of our model all the temperature-dependent data are consistent with the situation in which the residual ($T=0$) value of R_{EHE} and an almost linear slope of $R_{EHE,th}$ vs ρ_{th} curve is determined mainly by the core skew subsystem and the deviation from the linearity is due to a relatively small skew scattering contribution of the thermal disorder.

Both phonons and thermal spin disorder have been mentioned as possible sources of the EHE. Following Kagan and Maksimov[32] the phonon contribution is expected to be negligible as compared with that of magnons. However, our data provide no evidence for the role of magnons. At low temperatures the latter are expected to be suppressed by high magnetic fields ($T<15$ K for $B>15$ T). In our experiments, both Hall and longitudinal resistivity were measured up to 16.5 T and R_{EHE} was extrapolated from this high-field range. No change in behavior is marked when temperature is raised from 1.5K to room temperature. We are, therefore, inclined to believe that the observed modest temperature-dependent contribution to the EHE coefficient is due to phonons.

Temperature dependence of EHE in magnetic granular alloys has been recently treated by Granovsky *et al.*[33] Correlation of the type [Eq. (4)] has been predicted at high temperatures only above the Debye temperature, where resistivity is expected to vary linearly with temperature. It should be noted that we find a linear correlation between $R_{EHE,th}$ and ρ_{th} in the entire measured temperature range, including the low-temperature limit where resistivity saturates to its residual value [see Fig. 6(a)].

Few words need be added to justify our use of Matthiesen's rule. This phenomenological rule is widely accepted as a useful approximation by which the resistivity of metal can be presented as due to both the temperature-independent residual resistivity (due to defects) and phonon scattering. This assumption is valid if the two scattering mechanisms operate independently—that is the scattering by imperfections is temperature independent and there are insufficient imperfections to significantly affect the phonon scattering. The rule can be further subdivided if there is more than one type of imperfection (e.g., grain boundaries and surfaces,[23,34]). Deviations from Matthiesen's rule due to the interference terms are suppressed at high magnetic fields[35] which is the range we discuss. In heterogeneous magnetic systems, demonstrating the so-called giant magnetoresistance (GMR) effect, Matthiesen's rule is replaced by the two-current model representing a parallel flow of electrons with spins up and down. However, at high magnetic fields when magnetic moments of the system are aligned, the resistivity is given by: $1/\rho = 1/\rho_{\uparrow} + 1/\rho_{\downarrow}$, where $\rho_{\uparrow}$ and $\rho_{\downarrow}$ are resistivity of electrons with spins up and down, respectively. Large GMR effect is due to a large inequality of $\rho_{\uparrow}$ and $\rho_{\downarrow}$, and the high-field resistivity can be roughly approximated as due to one (lowest) component only: $\rho \approx \rho_{\downarrow}$. Therefore, Matthiesen's rule can be considered as valid in the high-field limit with only one type of carriers left.

Analysis proposed here might help to resolve several puzzles left by the traditional treatment of experimental data. We shall mention just few cases. Caulet *et al.*[27] studied the extraordinary Hall effect in Pt/Au/Co/Pt sandwiches with variable width of the Au layer. The authors tested the validity of Eq. (1) and noticed several unexpected features: (i) despite the high resistivity of their samples the skew scattering contribution $a\rho$ was always dominant; (ii) while coefficient a was found to increase slightly with thickness of gold layer, coefficient b decreased strongly and even changed sign. We have reexamined the same data by separating the residual and the temperature-dependent components. The temperature-dependent terms of all three samples have been found to collapse on a single curve following Eq. (4) with $a=0.95\pm0.05$ and $b=0.08\pm0.05$. The difference between the samples lies in their residual low-temperature resistivity and not in the temperature-dependent terms.

The effect of interfacial roughness on EHE has been studied by Korevinski *et al.*[28] in a series of Fe-Cr multilayers. Experimental data have been collected as a function of temperature and approximated by $R_{EHE}=\alpha\rho^n$. For the "smoothest" sample one calculated $n\approx2.0$, while for the "roughest" sample $n\approx2.3$. The authors concluded that the $R_{EHE}\propto\rho^2$ relationship is not unique, larger n corresponds to increasing roughness and, therefore, larger roughness leads to stronger temperature dependence. Decomposition of the same data to the residual and temperature-dependent terms leads to a dif-

ferent conclusion: the temperature dependence is identical for all samples. There is no dependence of the thermal component on roughness, which is consistent with our conclusions about the surface scattering component in Ni films (see Fig. 5).

In one of the first and widely cited works on transport properties of granular ferromagnets, P. Xiong *et al.*[15] reported a surprisingly high index $n=3.7$ in a power-law correlation $\rho_{EHE}=\alpha\rho^n$ between the Hall coefficient and longitudinal resistivity of a granular Co-Ag system. The data were accumulated by thermal treatment of samples with a constant volume concentration of Co at different annealing temperatures. Annealing affects the system in many ways: Co crystallizes, grains coalesce, their size increases, and density of clusters decreases, respectively. Simultaneously, dislocations in the matrix are healed and resistivity decreases. Nevertheless, following the common tradition, none of these details have been treated separately and only the overall final resistivity has been correlated with the total Hall effect. The power index 3.7 emerged and stimulated new theoretical efforts.[13] Accurate separation of parameters in the framework of our model is impossible in this experiment; however, the overall interpretation might be quite simple. An average size of Co clusters has been observed to grow with annealing from 2 nm to 13 nm. The volume density of Co clusters has, therefore, reduced roughly by a factor of 300, which is consistent with the observed reduction of ρ_{EHE}, uncorrelated to the change of resistivity.

It is an almost general perception that low-resistivity systems can be treated by the skew scattering model, whereas the side jump model must be applied in all other cases. One of many examples is another influential theoretical work by Shufeng Zhang[11] which concentrates on the side jump as the main source for the EHE in multilayered structures because their resistivities are usually much larger than that of individual bulk materials. It seems, however, that the total resistivity might be an erroneous parameter in particular when its significant part is contributed by scattering with negligible spin-orbit interaction. We were successful in analyzing much of experimental data using the skew scattering mechanism only. The analysis was successful also in high-resistivity systems where the side jump mechanism is automatically taken as the only dominating source of the EHE.

IV. SUMMARY

To summarize, we have abandoned the traditional comparison of the total values of the extraordinary Hall resistivity and longitudinal resistivity. Instead, we analyzed the correlation between the two parameters by decomposing them to contributions generated by different scattering sources. Two types of scattering sources have been distinguished: (i) skew sources that give rise to skew scattering, and (ii) ballast sources that do not generate skew scattering by themselves but contribute linearly to the EHE when additional skew sources are present. The extraordinary Hall effect is obtained as a combination of resistivity terms of both types of sources. Insulating impurities and surfaces are identified as ballast scattering sources. The temperature-dependent contribution, probably that of phonons, can be considered as close to being ballast with a relatively small self-skew scattering. All data discussed, measured in a variety of magnetic materials both new and previously published, can be fairly interpreted in the framework of the proposed modified skew scattering model without involving the quantum side jump mechanism.

ACKNOWLEDGMENTS

We acknowledge stimulating discussions with A. Palevski, R. Mints, and Y. Korenblit. This work has been supported in part by AFIRST Grant No. 9841 and by the Israel Science Foundation Grant No. 220/02.

[1] G. Bergman, Phys. Today **32**(8), 25 (1979).
[2] A. Gerber, A. Milner, M. Karpovski, B. Lemke, H.-U. Habermeier, J. Tuaillon-Combes, M. Négrier, O. Boisron, P. Mélinon, and A. Perez, J. Magn. Magn. Mater. **242–245**, 90 (2002), and references therein.
[3] J. E. Hirsch, Phys. Rev. B **60**, 14 787 (1999).
[4] R. Karplus and J. M. Luttinger, Phys. Rev. **95**, 1154 (1954).
[5] J. Smit, Physica (Amsterdam) **21**, 877 (1955).
[6] L. Berger, Phys. Rev. B **2**, 4559 (1970).
[7] J. Kondo, Prog. Theor. Phys. **27**, 772 (1962).
[8] F. E. Maranzana, Phys. Rev. **160**, 421 (1967).
[9] For review see, e.g., C. M. Hurd, *The Hall Effect in Metals and Alloys* (Plenum Press, New York 1972), p. 153; *The Hall Effect and its Applications*, edited by C. L. Chien and C. R. Westgate (Plenum Press, New York 1980), and references therein.
[10] J. M. Luttinger, Phys. Rev. **112**, 739 (1958).
[11] S. Zhang, Phys. Rev. B **51**, 3632 (1995).
[12] A. Granovsky, F. Brouers, A. Kalitsov, and M. Chshiev, J. Magn. Magn. Mater. **166**, 193 (1997).
[13] A. V. Vedyaev, A. B. Granovsky, A. V. Kalitsov, and F. Brouers, JETP **85**, 1204 (1997).
[14] S. N. Song, C. Sellers, and J. B. Ketterson, Appl. Phys. Lett. **59**, 479 (1991).
[15] P. Xiong, G. Xiao, J. Q. Wang, J. Q. Xiao, J. S. Jiang, and C. L. Chien, Phys. Rev. Lett. **69**, 3220 (1992).
[16] J. M. Lavine, Phys. Rev. **123**, 1273 (1961).
[17] J. A. Dreesen and E. M. Pugh, Phys. Rev. **120**, 1218 (1960).
[18] R. Malmhall, G. Backstrom, S. M. Bhagat, and K. V. Rao, J. Non-Cryst. Solids **28**, 159 (1978).
[19] A. Perez *et al.*, J. Phys. D **30**, 709 (1997).
[20] M. Jamet, M. Négrier, V. Dupuis, J. Tuaillon-Combes, P. Mélinon, A. Pérez, W. Wersdorfer, B. Barbara, and B. Baguenard, J. Magn. Magn. Mater. **237**, 293 (2001).
[21] A. Gerber, A. Milner, L. Goldsmith, M. Karpovski, B. Lemke, H.-U. Habermeier, and A. Sulpice, Phys. Rev. B **65**, 054426 (2002).
[22] E. H. Sondheimer, Adv. Phys. **1**, 1 (1959).
[23] A. Milner, A. Gerber, B. Groisman, M. Karpovsky, and A. Glad-

kikh, Phys. Rev. Lett. **76**, 475 (1996).
[24] C. Vautier, J. Phys. (France) **27**, 531 (1966).
[25] S. J. Raeburn and R. V. Aldridge, J. Phys. F: Met. Phys. **8**, 1917 (1978).
[26] J. P. Jan, Helv. Phys. Acta **25**, 677 (1952).
[27] J. Caulet, C. Train, V. Mathet, R. Laval, B. Bartenlian, P. Veillet, K. Le Dang, C. Chappert, J. Magn. Magn. Mater. **198–199**, 318 (1999).
[28] V. Korenivski, K. V. Rao, J. Colino, and I. K. Schuller, Phys. Rev. B **53**, R11938 (1996).
[29] F. Tsui, B. Chen, D. Barlett, R. Clarke, and C. Uher, Phys. Rev. Lett. **72**, 740 (1994).
[30] Y. Kobayashi, K. Honda, Y. Aoki, H. Sato, T. Ono, Y. Shinjo, S. A. Makhlouf, K. Sumiyama, K. Suzuki, J. Magn. Magn. Mater. **176**, 164 (1997).
[31] C. L. Canedy, X. W. Li, and G. Xiao, Phys. Rev. B **62**, 508 (2000).
[32] Yu. Kagan and L. A. Maksimov, Sov. Phys. Solid State **7**, 422 (1965).
[33] A. Granovsky, A. Kalitsov, A. Khanikaev, H. Sato, and Y. Aoki, J. Magn. Magn. Mater. **257**, 306 (2003).
[34] A. F. Mayadas and M. Shatzkes, Phys. Rev. B **1**, 1382 (1970).
[35] Yu. Kagan and V. N. Flerov, Sov. Phys. JETP **39**, 673 (1974).